DEUTSCHES ELEKTRONEN – SYNCHROTRON DESY

DESY 87-108
August 1987

COMPOSITENESS IN EP COLLISIONS AT LEP-LHC

by

F. Cornet, R. Rückl

Deutsches Elektronen-Synchrotron DESY, Hamburg

ISSN 0418-9833

NOTKESTRASSE 85 · 2 HAMBURG 52

DESY 87-108
August 1987

ISSN 0418-9833

COMPOSITENESS IN EP COLLISIONS AT LEP-LHC*

F. Cornet and R. Rückl

Deutsches Elektronen-Synchrotron DESY, Hamburg, Fed.Rep. of Germany

* Contribution to the Workshop on Physics at Future Accelerator,
La Thuile and CERN, 1987

COMPOSITENESS IN EP COLLISIONS AT LEP-LHC

F. Cornet and R. Rückl

Deutsches Elektronen-Synchrotron DESY, Hamburg, Fed. Rep. of Germany

ABSTRACT

If leptons and quarks are composite one expects, among other signals, the occurrence of excited states and non-renormalizable residual interactions. We have studied electron quark contact interactions and the production of excited electrons in collisions of an electron (or positron) beam of LEP with a proton beam of the LHC. Estimates are presented for the sensitivity to the effective scale Λ_{eq} of contact terms with varying helicity structure, and for the detection limit in the mass m_{e^*} of a heavy replica of the ground state electron.

1. INTRODUCTION

Composite Models [1,2] are motivated by the mass problem and the generation puzzle of the Standard Model which find expression in many unexplained parameters. Several levels of compositeness have been considered: composite Higgs scalars, composite leptons and quarks, and even composite weak bosons. Here, we focus on the possibility that leptons and quarks are bound states of more fundamental constituents. The binding force should probably be confining at a scale Λ in which case the bound state radius r is expected to be of order $1/\Lambda$. Clearly, Λ cannot be too small without running into contradictions with experimental results [3]. It seems, however, that values of Λ in the TeV range are not yet excluded by experiment if one assumes that pitfalls such as the very stringent bounds on lepton number and flavor violating processes [4] can somehow be avoided. In addition, a consistent theory must explain why the known leptons and quarks are so light, that is why $m_{l,q} \ll \Lambda \sim 1/r$ quite in contrast to our experience with ordinary QCD bound states such as the ρ meson and the nucleon. Notwithstanding the problems and short-comings of present Composite Models, searches for a new substructure obviously belong to the main tasks at future colliders.

At energies $E > \Lambda$ the composite nature of leptons and quarks should become evident through break-up of the bound states in hard scattering processes, and through the production of excited states with masses $m = O(\Lambda)$. However, one may also observe some indications already at energies $E < \Lambda$, such as deviations from the Standard Model predictions due to form factors and residual interactions induced by the binding force. The present study deals with possibilities of unveiling compositeness in electron-proton collisions at energies just above 1 TeV. We have concentrated our attention on effects from electron-quark contact interactions and the production of excited electrons. Searches for these signals are sensitive to relatively large values of the compositeness scale Λ and thus provide favorable tests at high-energy ep colliders [5].

The ep machine envisaged is a combination of LEP and LHC, the hadron collider in the LEP tunnel. As discussed at this workshop [6], it would be possible to provide collisions of a $(50 - 100)$ GeV electron or positron beam of LEP with a 8 TeV proton beam of LHC yielding the typical c.m. energies and luminosities,

$$\begin{array}{lll} \text{(I)} & \sqrt{s} = 1.4\, TeV \quad \text{and} & L = 10^{32}\, cm^{-2} s^{-1}, \\ \text{(II)} & \sqrt{s} = 1.8\, TeV \quad \text{and} & L = 10^{31}\, cm^{-2} s^{-1}. \end{array} \tag{1}$$

We give priority to option (I) for two reasons: the higher luminosity and the possibility to have longitudinally polarized $e^{\pm}$ beams at LEP I. These virtues increase the discovery potential for option (I) quite considerably as compared to the higher energy option. A summary of our results has been presented in the report by J. Ellis and F. Pauss [7].

2. ELECTRON-QUARK CONTACT INTERACTIONS

An essentially unavoidable consequence of compositeness are residual interactions described by non-renormalizable operators in the effective low-energy lagrangian [8,9]. The most important ones are four-fermion operators which have dimensionful coupling constants proportional to g_{eff}^2/Λ^2 where Λ is the binding scale. Furthermore, since the binding force is expected to be strong, it is plausible to assume that the effective coupling $g_{eff}^2/4\pi = O(1)$. Interferences between such contact interactions and conventional gauge interactions lead to deviations from Standard Model expectations which are observable at energies considerably below Λ. In fact, from Bhabha scattering at PETRA and PEP one has obtained limits on ee contact terms in the range [3]

$$\Lambda_{ee} \geq 1 - 3\ TeV, \tag{2}$$

while high-p_T jet production at the CERN $\bar{p}p$ Collider [10] has constrained possible qq contact interactions to

$$\Lambda_{qq} \geq 450\ GeV. \tag{3}$$

We are not aware of published bounds for lepton-quark contact terms which could be tested in e^+e^- annihilation into hadrons, Drell-Yan processes, and lepton-nucleon scattering. In order to keep the effects on neutrino cross-sections below 10% one roughly needs $\Lambda_{\nu q} \geq 2\ TeV$. Future experiments at HERA are expected [11,12] to be sensitive to values of Λ_{eq} up to

$$\Lambda_{eq} \simeq 5\ TeV. \tag{4}$$

One can thus anticipate that ep collisions at TeV energies should allow to search for eq contact interactions in the range $\Lambda_{eq} = O(10\ TeV)$. This assertion is substantiated and made more quantitative in the following.

2.1 Definition of Models

Restricting ourselves to the neutral current (NC) processes $e^{\pm}p \rightarrow e^{\pm}X$, we have considered models based on the effective lagrangian

$$\mathcal{L}_{eff} = \mathcal{L}_{SM} + \mathcal{L}', \tag{5}$$

where

$$\mathcal{L}_{SM} = e\sum_f \bar{f}\gamma^\mu Q_f f A_\mu + \frac{e}{\sin\theta_W \cos\theta_W}\sum_f \bar{f}\gamma^\mu(v_f - a_f\gamma_5)fZ_\mu \tag{6}$$

and

$$\begin{aligned}\mathcal{L}' = \textstyle\sum_q\{g^2_{eff}\ &[(\eta_{LL}/\Lambda^2_{LL})(\bar{e}_L\gamma^\mu e_L)(\bar{q}_L\gamma^\mu q_L) + (\eta_{RR}/\Lambda^2_{RR})(\bar{e}_R\gamma^\mu e_R)(\bar{q}_R\gamma^\mu q_R)\\ &+(\eta_{LR}/\Lambda^2_{LR})(\bar{e}_L\gamma^\mu e_L)(\bar{q}_R\gamma^\mu q_R) + (\eta_{RL}/\Lambda^2_{RL})(\bar{e}_R\gamma^\mu e_R)(\bar{q}_L\gamma^\mu q_L)]\}.\end{aligned} \tag{7}$$

$\mathcal{L}_{SM}$ is the standard NC lagrangian which , at low energies, describes the gauge interactions of the photon and the Z boson with the electron and the quarks. At momentum scales $Q^2 \ll \Lambda^2$ the fermions appear pointlike and hence one may neglect modifications of the gauge couplings due to form factors. The following notation is used in eq.(6): el.magn. coupling e, Weinberg angle θ_W, el.magn. charge Q_f with the convention $Q_e = -1$, third component of weak isospin T_{3f} with the convention $T_{3e} = -1/2$, vector coupling $v_f = T_{3f}/2 - Q_f \sin^2\theta_W$ and axial vector coupling $a_f = T_{3f}/2$. For consistency, the values of the electroweak parameters should be determined in the present models by confronting $\mathcal{L}_{eff}$ with the low-energy CC and NC data and with W and Z mass measurements. However, if $\Lambda >$ few TeV, the result will practically be the same as for the Standard Model. It is therefore justified to assign the usual values to the NC parameters in the later applications of $\mathcal{L}_{eff}$. We have taken $\alpha = e^2/4\pi = 1/137$, $m_Z = 93.3\ GeV$ and $\sin^2\theta_W = (1-(1-4\mu^2/m_Z^2)^{1/2})/2$ with $\mu = 38.65\ GeV$.

New in eq.(5) is the effective lagrangian $\mathcal{L}'$ describing residual four-fermion interactions which conserve helicity and flavor, and are therefore expected to be only suppressed by the binding scale Λ_{eq}. (For simplicity, we often use the shorthand Λ_{eq} for the different scales Λ_{LL}, Λ_{RR}, etc...) Following ref.[8], where the form of $\mathcal{L}'$ assumed in eq.(7) was suggested, we use the conventions $g^2_{eff}/4\pi = 1$ and $\eta_{ab} = \pm 1$ or 0 for $a, b = L, R$. As illustrative examples, we have investigated the simple cases defined in Table 1. Our study is guided by ref.[11] where these models are discussed in detail in the context of searches for eq contact terms at HERA.

Table 1

Models for eq contact terms considered in the present study

$\epsilon = \pm 1$	LL	LR	RL	RR	VV	AA
η_{LL}	ϵ	0	0	0	ϵ	ϵ
η_{LR}	0	ϵ	0	0	ϵ	$-\epsilon$
η_{RL}	0	0	ϵ	0	ϵ	$-\epsilon$
η_{RR}	0	0	0	ϵ	ϵ	ϵ

For clarity, we should remark that inclusive observables are calculated throughout this paper by summing over u, d, s and c quark flavors in the proton, using set I of the Duke-Owens quark distribution functions [13]. Since contact terms can be interpretated as being induced by interchange of common subconstituents of leptons and quarks, it may be more conservative to restrict such interactions in the case of ep scattering to u and d quark flavors [8,11]. While in any sensible Composite Model the members of one and the same fermion family should be made of common building blocks, the substructure and binding scales could be very different for the different families. In fact, in view of the extremely severe bounds on flavor violating transitions from rare processes [4] this possibility appears quite likely. The conclusions which can be drawn from our estimates would however not change if we omitted es and ec contact terms.

2.2 Cross-Sections and Asymmetries

From the effective lagrangian $\mathcal{L}_{eff}$ given in eq.(5) one readily derives the differential cross-sections $d\sigma(e^{\pm}p)/dxdQ^2$ for polarized $e^{\pm}p$ scattering. Here, $Q^2 = -k^2$ and $x = -k^2/2pk$, where k denotes the four-momentum exchanged in $eq \to eq$ and p is the incoming proton momentum. The relevant cross-section formulas can be found in ref.[14] of these Proceedings (see eqs.(14-16) and (20)). Here, it is therefore sufficient to provide the effective charge coefficients $\tilde{F}_{2f}^{L,R}$ and $\tilde{F}_{3f}^{L,R}$ which are to be substituted in equations (15) and (16) of ref.[14]. These coefficients read

$$\begin{aligned} \tilde{F}_{2f}^{L,R} &= [V_f^{L,R}(Q^2)]^2 + [A_f^{L,R}(Q^2)]^2, \\ \tilde{F}_{3f}^{L,R} &= 2V_f^{L,R}(Q^2)A_f^{L,R}(Q^2), \end{aligned} \tag{8}$$

with

$$V_f^{L,R}(Q^2) = Q_f - \frac{(v_e \pm a_e)v_f}{\cos^2\theta_W \sin^2\theta_W}\left(\frac{Q^2}{Q^2+m_Z^2}\right) + c^{L,R}\frac{Q^2}{2\alpha\,\Lambda^2}, \tag{9}$$

$$A_f^{L,R}(Q^2) = \mp\frac{(v_e \pm a_e)a_f}{\cos^2\theta_W \sin^2\theta_W}\left(\frac{Q^2}{Q^2+m_Z^2}\right) \pm d^{L,R}\frac{Q^2}{2\alpha\,\Lambda^2}. \tag{10}$$

The numbers $c^{L,R}$ and $d^{L,R}$ are given in Table 2 for the models specified in Table 1, while the remaining parameters are explained in paragraph 2.1.

Table 2

Model parameters of contact terms to be substituted in eqs.(9) and (10)

$\epsilon = \pm 1$	LL	LR	RL	RR	VV	AA
c^L	ϵ	ϵ	0	0	2ϵ	0
d^L	ϵ	$-\epsilon$	0	0	0	2ϵ
c^R	0	0	ϵ	ϵ	2ϵ	0
d^R	0	0	ϵ	$-\epsilon$	0	2ϵ.

Besides cross-sections, we have also investigated the NC asymmetries

$$A(e_1 - e_2) = \frac{\tilde{\sigma}(e_1) - \tilde{\sigma}(e_2)}{\tilde{\sigma}(e_1) + \tilde{\sigma}(e_2)}, \tag{11}$$

where $\tilde{\sigma}(e_i)$ denotes either the doubly differential cross-section $d\sigma(e_ip)/dxdQ^2$ or the cross-section $d\sigma(e_ip)/dQ^2$ obtained after integration over x. With the four polarization states $e_i = e^{\pm}_{L,R}$ one can construct six different asymmetries: the polarization asymmetries $A(e^-_L - e^-_R)$ and $A(e^+_L - e^+_R)$, the charge asymmetries $A(e^-_L - e^+_L)$ and $A(e^-_R - e^+_R)$, and the mixed asymmetries $A(e^-_L - e^+_R)$ and $A(e^-_R - e^+_L)$.

2.3 Signals and Detection Limits

2.3.1 Unpolarized cross-sections

The simplest way to test eq contact interactions is to compare Q^2-distributions measured in unpolarized $e^{\mp}p$ collisions with the predictions of the Standard Model. Figs. 1 and 2 illustrate possible deviations in the cross-sections

$$\sigma_{ij}(e^{\mp}p) = \int_{Q_i^2}^{Q_j^2} dQ^2 \int_{Q^2/s}^{1} dx \frac{d\sigma(e^{\mp}p)}{dxdQ^2} \tag{12}$$

for some selected contact terms, considering suitable bins in Q^2. Qualitatively, we find that the changes due to LL (LR) terms are similar to the changes due to RR (RL) terms. Furthermore, e^-p scattering is somewhat more sensitive to LL (and RR) contact interactions, whereas RL (and LR) contact terms show up more clearly in e^+p scattering. Finally, VV- and AA- type contact interactions produce the largest effects and can be best probed in e^+p scattering except in the case of VV($\epsilon = +1$) terms where the e^-p cross-section is more sensitive.

Indicative estimates for the sensitivity of searches for effects in inclusive NC cross-sections can be obtained by considering the statistical errors on $\sigma_{ij}(e^{\mp}p)$. For this purpose we assume a one-year run at $\sqrt{s} = 1.4\ TeV$ yielding an integrated luminosity of 1 fb^{-1} shared equally between $e^{\pm}$ beams. The corresponding statistical errors are displayed in Figs. 1 and 2. At lower values of Q^2 the Standard Model is expected to agree with experiment to a rather high accuracy. A comparison in this region should thus allow to reduce theoretical uncertainties and systematic errors (e.g. in luminosity measurements and determinations of Q^2). The data at higher values of Q^2 could then be used to test the presence of contact interactions. Instead of performing a full χ^2-analysis, we shall only look at the highest Q^2-bin shown in Figs. 1 and 2, where the statistical error on the Standard Model cross-sections amounts to $\delta\sigma_{ij}(e^{\mp}p)/\sigma_{ij}(e^{\mp}p) \simeq 4\%$. Requiring possible deviations to be at least as large as the statistical error, one can reach the values of Λ_{eq} summarized in Table 3 for the models under consideration. With the same criterion but for an experimental uncertainty which is arbitrarily increased by a factor 2 in order to allow for some systematic errors, the sensitivity to Λ_{eq} decreases as also indicated in Table 3.

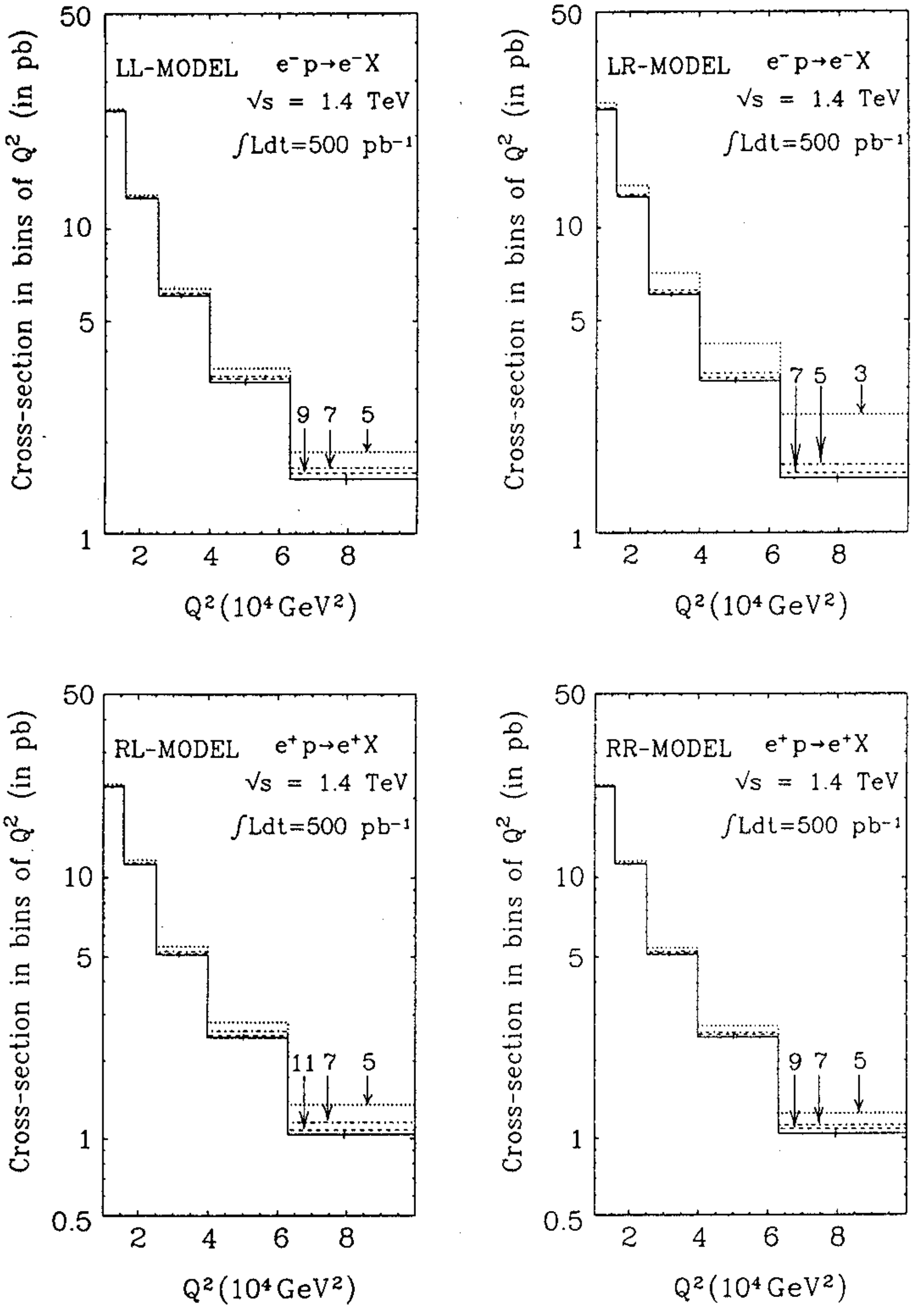

Fig. 1 Neutral current cross-sections integrated over x for contact interactions with $\epsilon = +1$ in comparison to the Standard Model predictions (full lines). The numbers labelling the curves give the scales Λ_{eq} in TeV. The statistical errors refer to a total integrated luminosity of $1 fb^{-1}$ shared equally between $e^{\mp}\ p$ collisions.

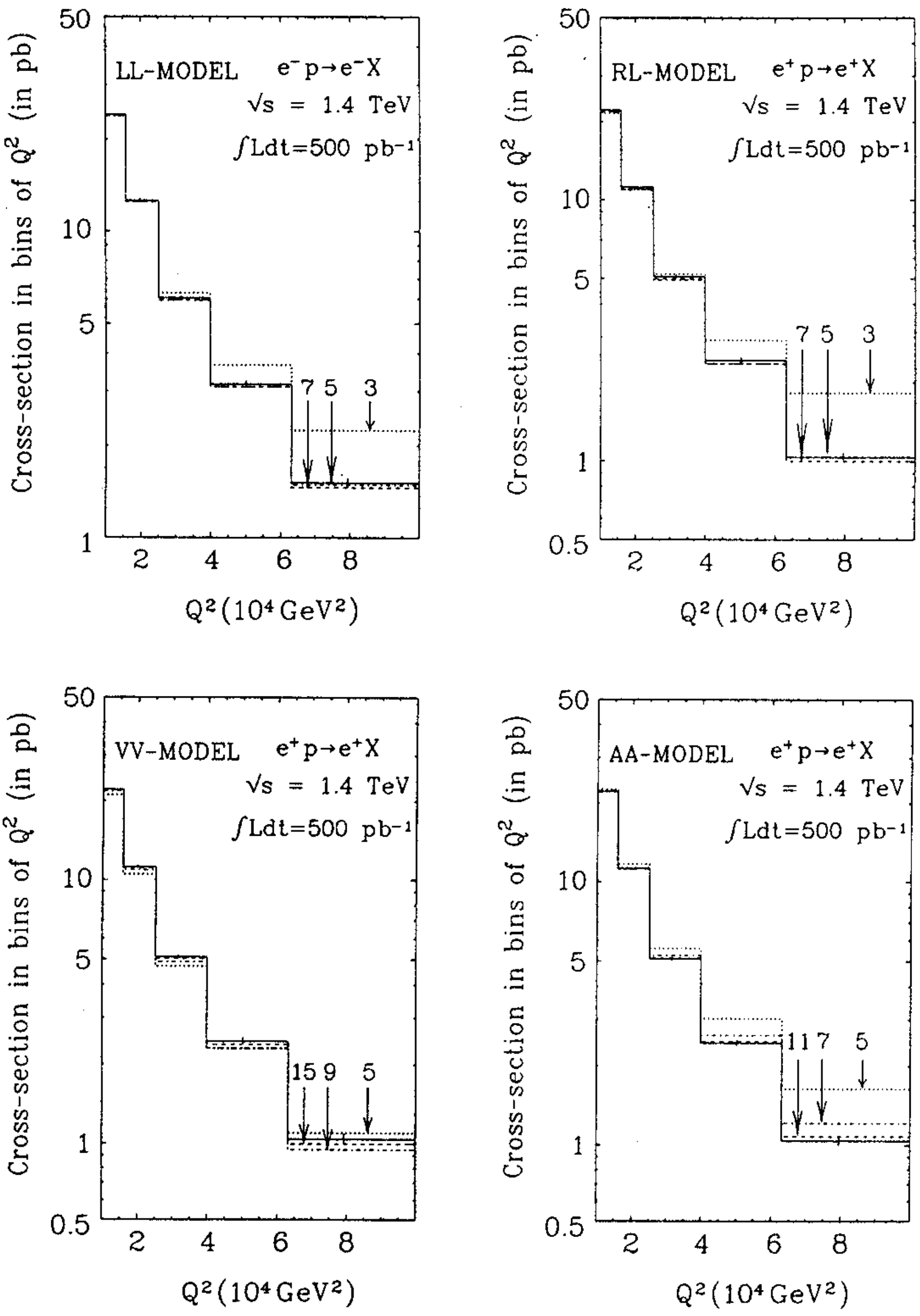

Fig. 2 Same as in Fig. 1 for a different selection of the contact terms and $\epsilon = -1$.

Table 3

Estimates for the sensitivity to eq contact interactions in measurements of unpolarized NC cross-sections at $\sqrt{s} = 1.4\,TeV$. The experimental errors assumed refer to the Q^2-bin from $6 \times 10^4\ GeV^2$ to $10^5 GeV^2$

Model	$\Lambda_{eq}(TeV)$	
$(\epsilon = +1)$	$(\delta\sigma/\sigma)_{stat} \simeq 4\%$	$\delta\sigma/\sigma \simeq 8\%$
LL	9	7
LR	9	7
RL	10	8
RR	10	7
VV	16	12
AA	11	9

We have only quoted estimates for models with $\epsilon = +1$, that is for positive values of the effective couplings η_{ab} in eq.(7). For $\epsilon = -1$ one has to perform a more involved analysis since the deviations may change the sign at some value of Q^2 due to a more complicated interference pattern. As a consequence, if one only looks at a particular bin in Q^2, there may be no effect for a given value of Λ_{eq} and a sizable effect for another, larger value of Λ_{eq}. This actually happens in some of the cases illustrated in Fig. 2. Generally, one can say that the values of Λ_{eq} which can be reached for $\epsilon = -1$ are markedly lower than the ones for $\epsilon = +1$.

Finally, we have also considered ep collisions at $\sqrt{s} = 1.8\,TeV$ and $L = 10^{31}\ cm^{-2}s^{-1}$ and find considerable lower sensitivity limits for Λ_{eq} than at $\sqrt{s} = 1.4\ TeV$ and $L = 10^{32}\ cm^{-2}s^{-1}$. This shows that luminosity plays a more important role in searches for contact terms than energy.

2.3.2 Asymmetries

It is not unlikely that longitudinal $e^{\pm}$ polarization can be attained at LEP I. In that case, the LEP-LHC ep option could provide polarized $e^{\mp}p$ collisions at $\sqrt{s} = 1.4\ TeV$. Therefore, we have also studied the prospects for disclosing contact interactions in asymmetry measurements. Figs. 3 and 4 illustrate the changes in NC asymmetries due to eq contact terms for all types of asymmetries introduced in eq.(11), and for all models defined in Tables 1 and 2. We have chosen $\Lambda_{eq} = 5\ TeV$, since this value characterizes the limit of observability at HERA. From Figs. 3 and 4 one can learn several interesting facts:

(1) NC asymmetries are very sensitive to the helicity structure of contact interactions and are therefore useful for determining the residual couplings, if a signal is observed.

(2) For each model considered one can find one or several asymmetries which are particularly sensitive. Reversely, a measurement of all asymmetries guarantees an appreciable sensitivity to contact terms for any helicity combination.

(3) The influence of contact terms depends crucially on the relative sign (parameterized by $\epsilon = \pm 1$) of the residual lagrangian $\mathcal{L}'$ and the lagrangian $\mathcal{L}_{SM}$ describing the standard gauge interactions. This underlines that the signals mainly come from interferences.

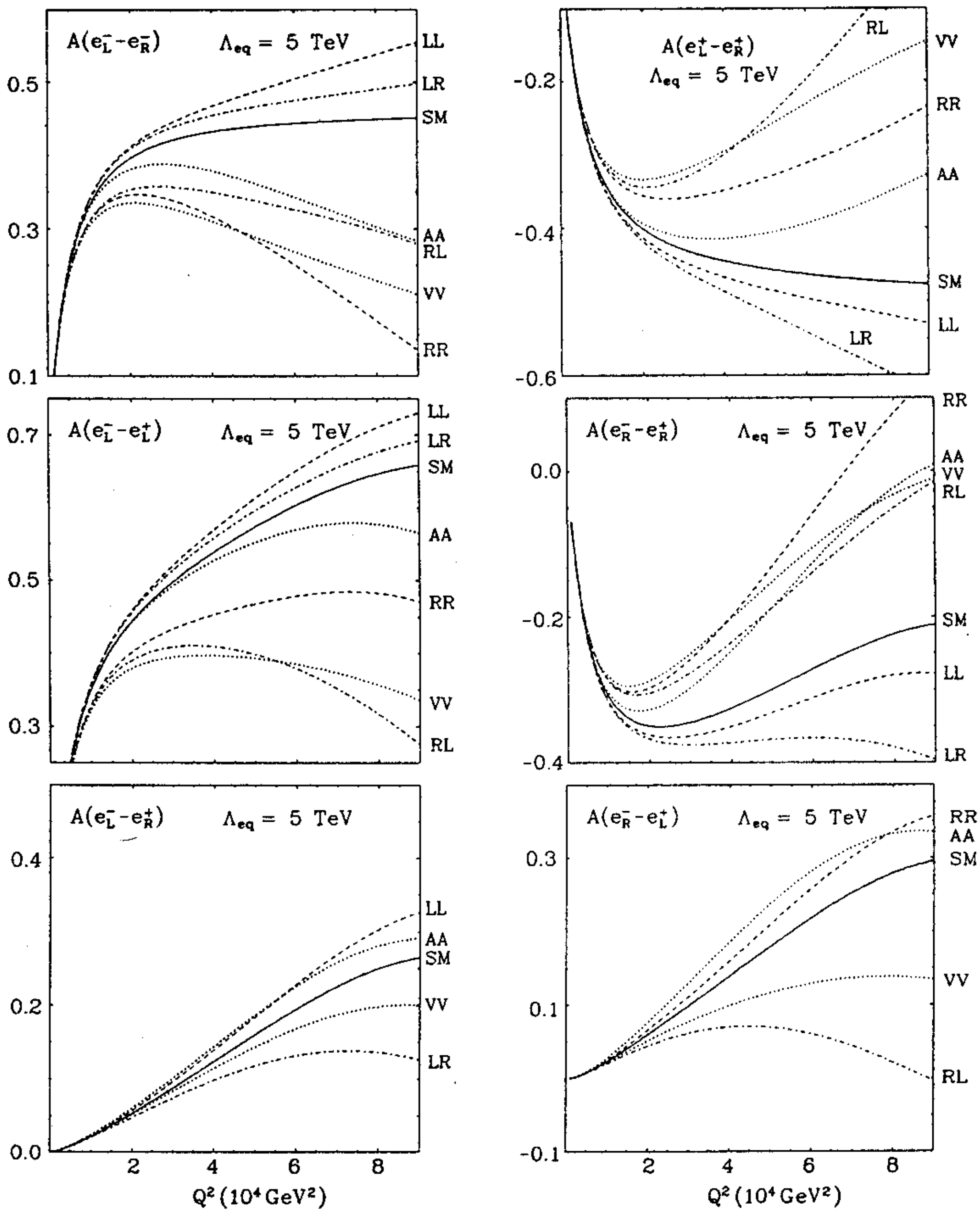

Fig. 3 Neutral current asymmetries at $\sqrt{s} = 1.4\ TeV$ and $x = 0.05$ for contact interactions with $\epsilon = +1$, assuming $\Lambda_{eq} = 5\ TeV$. Also shown are the Standard Model expectations (SM).

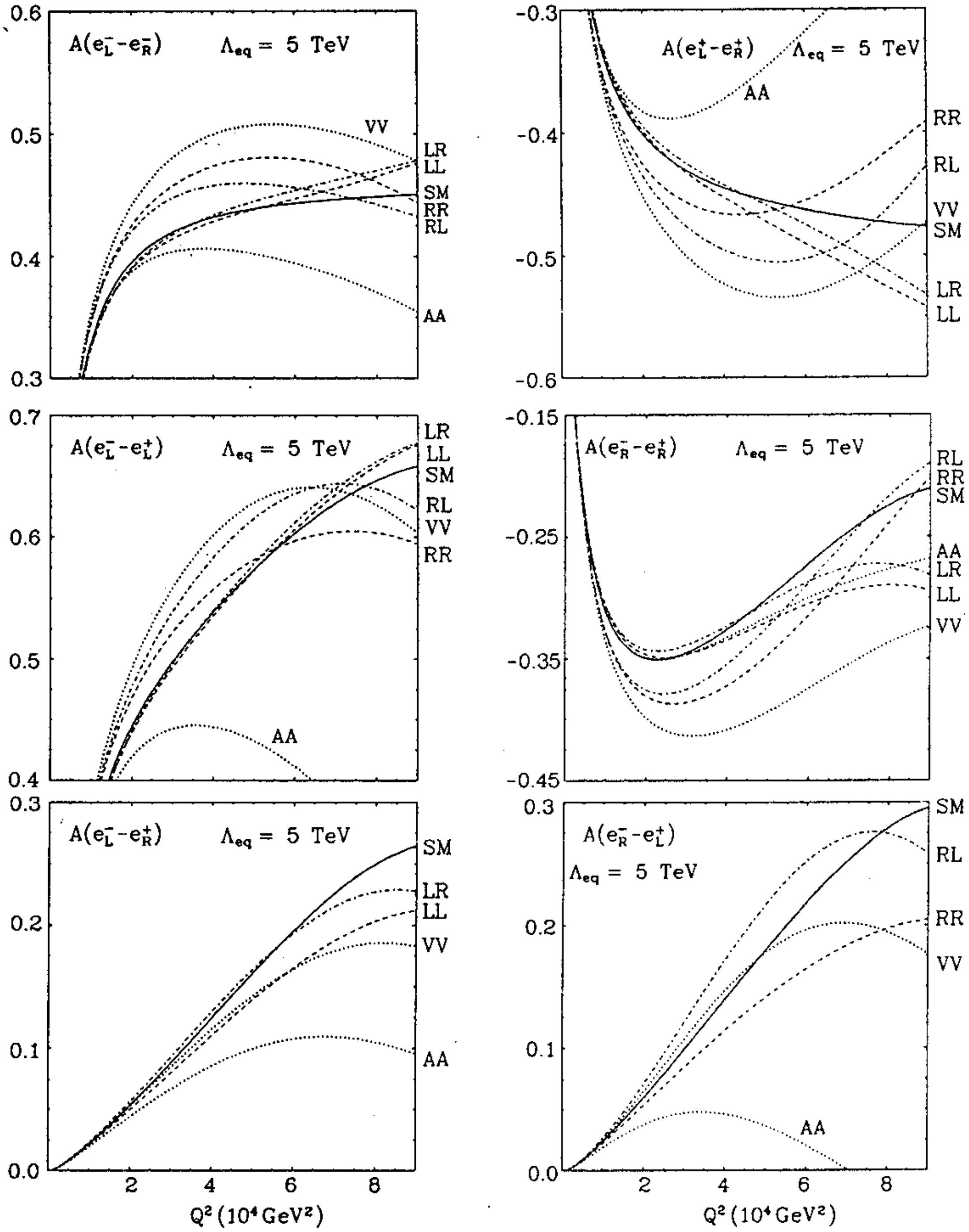

Fig. 4 Same as Fig. 3 but for $\epsilon = -1$.

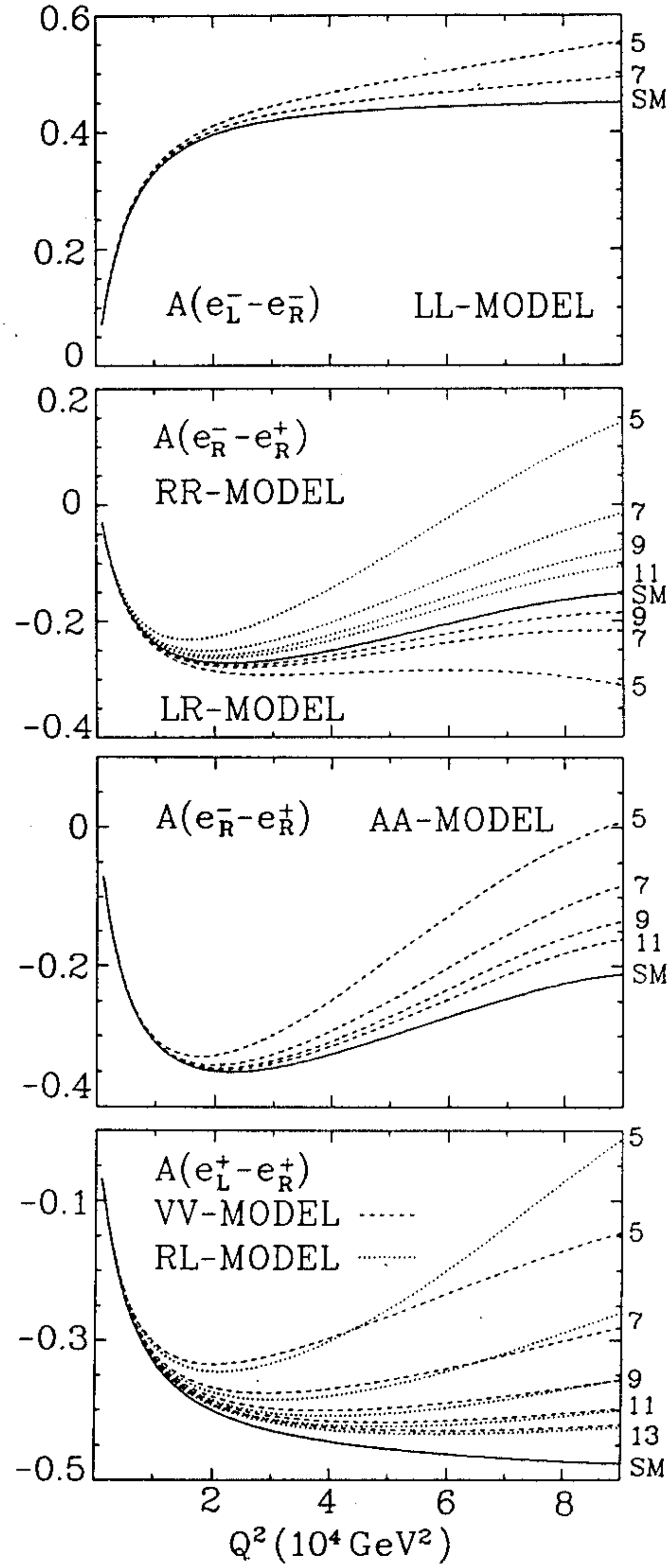

Fig. 5 Expected deviations from the Standard Model predictions (SM) at $\sqrt{s} = 1.4\ TeV$ and $x = 0.05$ for various values of Λ_{eq} (in TeV) and $\epsilon = +1$. For each type of contact term the most sensitive asymmetry is plotted.

Next we select, from Fig. 3, the most sensitive asymmetry (called "best" further on) for each model, considering only the favorable case $\epsilon = +1$. We then increase Λ_{eq} in order to get an approximate idea of the maximum values of Λ_{eq} which may be reached. This exercise is shown in Fig. 5. One can see that for Λ_{eq} in the range $(7-13)\ TeV$ the best asymmetries deviate at the largest values of Q^2 by roughly $(10-30)\%$ from the Standard Model expectations.

Table 4

Estimates for the sensitivity to eq contact interactions in asymmetry measurements at $\sqrt{s} = 1.4\,TeV$. The statistical error refers to the Q^2-bin from $6 \times 10^4\ GeV^2$ to $10^5 GeV^2$

Model $\epsilon = +1$	most sensitive asymmetry	$\Lambda_{eq}\ (TeV)$ $\delta A_{stat} \simeq 0.04$
LL	$e_L^- - e_R^-$	8
LR	$e_L^- - e_R^-$	9
RL	$e_L^+ - e_R^+$	13
RR	$e_R^- - e_R^+$	13
VV	$e_L^+ - e_R^+$	14
AA	$e_R^- - e_R^+$	11

As in the previous analysis for the NC cross-sections, we have estimated the sensitivity to contact terms by comparing possible deviations to statistical errors. Again, we refer to an integrated luminosity of 1 fb^{-1} assuming $250pb^{-1}$ for each of the four polarization states $e^{\mp}_{L,R}$. In Fig. 6 expectations for the different contact interactions (taking $\epsilon = +1$) are confronted with the predictions of the Standard Model including the statistical errors. In all cases we have considered the most sensitive asymmetry as suggested by Fig. 5. In order to increase the number of events in the Q^2-bins, the $e^{\mp}_{L,R}$ cross-sections entering in eq.(11) have been integrated over x. The values of Λ_{eq} chosen in Fig. 6 are supposed to indicate the expected sensitivity limits. Imposing the requirement that the deviations are at least as large as the statistical error at $Q^2 \simeq 6\times 10^4\ GeV^2$ to $10^5 GeV^2$, one can hope to probe contact interactions in asymmetry measurements up to the values of Λ_{eq} summarized in Table 4. Unfortunately we do not know the systematic errors. We believe, however, that some systematic errors cancel in asymmetries, which are basically cross-section ratios, while other uncertainties may be removed by comparing the Standard Model predictions with the data in the low Q^2 region where good agreement can be expected. Moreover, a complete χ^2-analysis would make the tests more significant than what can be inferred from Fig. 6.

3. EXCITED ELECTRONS

The interpretation of the known leptons and quarks as the ground state of a bound system naturally implies the existence of excited states. As a matter of fact, Composite Models usually predict excited leptons and quarks with both conventional and exotic quantum

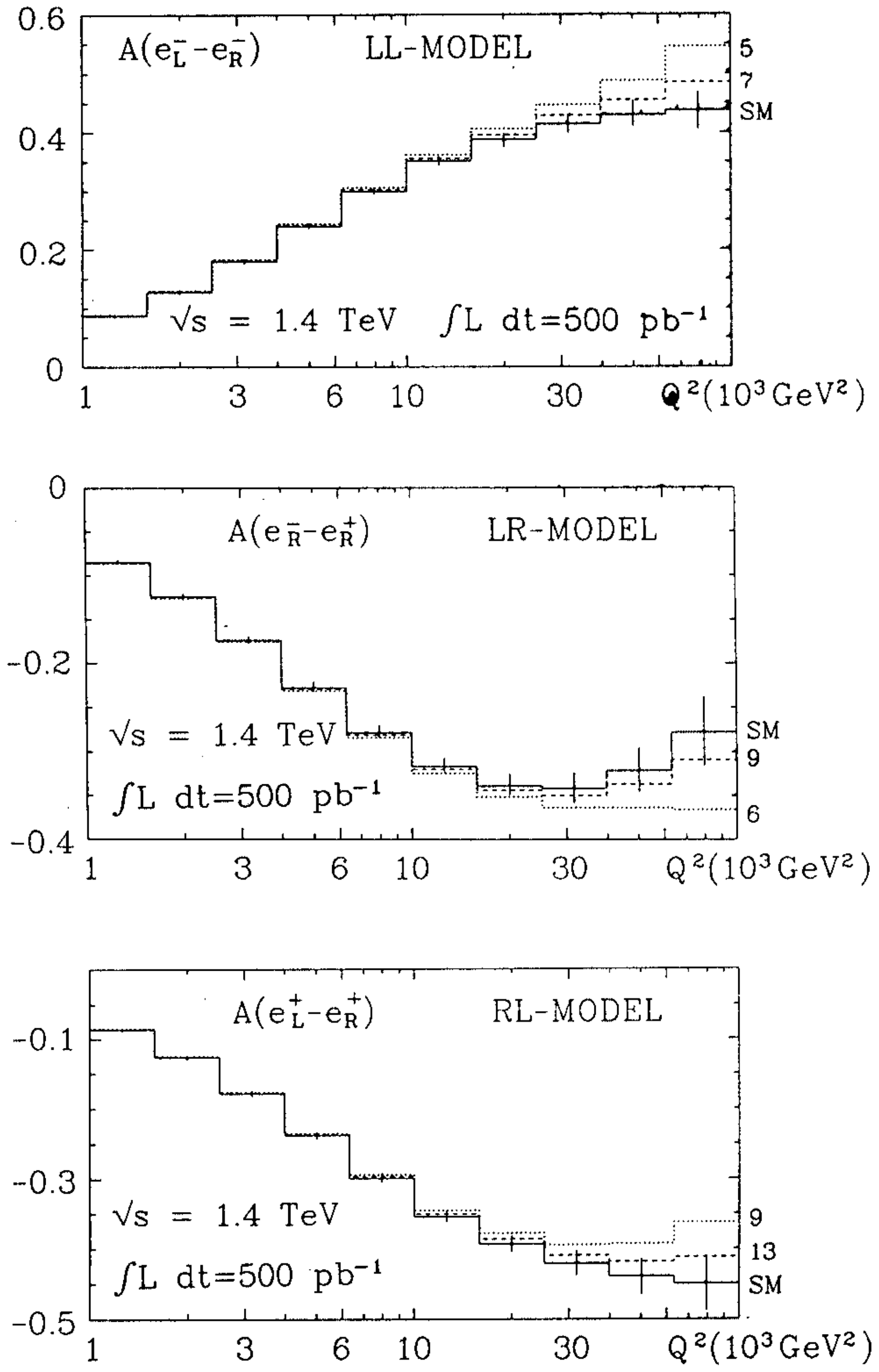

Fig. 6 Neutral current asymmetries integrated over x for contact terms with $\epsilon = +1$ in comparison to the Standard Model predictions (SM). The numbers labelling the curves give the values Λ_{eq} in TeV. The statistical errors are for a total integrated luminosity of $1 fb^{-1}$ shared equally among $e^{\mp}_{L,R}p$ collisions.

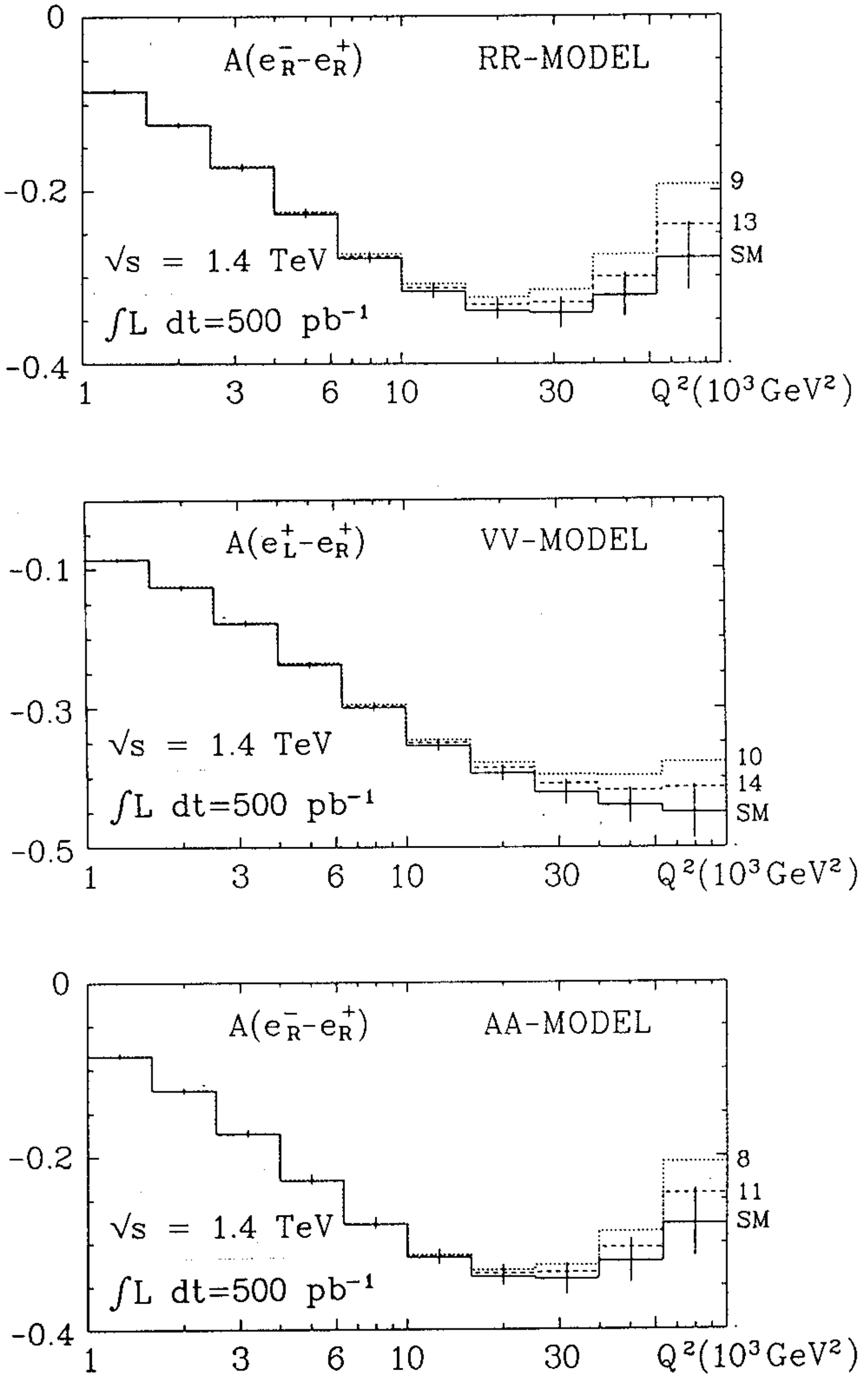

Fig. 6 (continued)

numbers (such as color-octet leptons and color-sextet quarks) [1,2]. Normally, these particles should have masses of the order of the binding scale Λ. Hence, if $\Lambda \geq$ few TeV as we assume, excited states would be out of experimental reach in ep collisions at LEP-LHC. However, it may well be that a similar mechanism which keeps the ground state fermions light as compared to the scale Λ, also leads to some relatively light excited states. This possibility is not excluded, at least, not experimentally. On the contrary, the current limits on the masses of excited fermions are rather weak. From e^+e^- annihilation, for example, one has obtained bounds in the range [3]

$$m_{e^*} \geq (23 - 70)\ GeV, \tag{13}$$

where only the lower limit is independent of assumptions on the coupling strength of the excited to the ground state electron.

The dominant sources of excited leptons and quarks in high-energy ep collisions are the single production processes $ep \to l^*X$ and $ep \to lq^*X$. Most promising is the search for an e^* because of relatively comfortable production rates and clean decay signatures [5,15,16]. For illustration of the discovery potential at LEP-LHC, we have considered an e^* state with the quantum numbers spin 1/2, $T_{3e^*} = -1/2$ and $Q_{e^*} = -1$, which belongs to a weak isospin doublet (ν^*, e^*). Production in $ep \to e^*X$ proceeds through γ and Z exchange and thus involves the unknown $ee^*\gamma$ and ee^*Z couplings. Gauge invariance requires these couplings to have the form of magnetic transitions, while dangerous contributions to the $g-2$ of the electron can be avoided if the couplings are restricted to one helicity component of the electron [17]. Hence, we assume the effective lagrangian [5,7,15]

$$\mathcal{L} = \frac{e}{2\Lambda^*}\bar{e}^*\sigma_{\mu\nu}e_L(A^{\mu\nu} + \frac{1-2\sin^2\theta_W}{\sin 2\theta_W}Z^{\mu\nu}), \tag{14}$$

where $A^{\mu\nu}$ and $Z^{\mu\nu}$ denote the photon and Z-boson field strengths, respectively, and Λ^* characterizes the typical excitation scale. For consistency with studies for other machines in these Proceedings [7], we shall take $\Lambda^* = m_{e^*}$ when presenting numerical results, although the two parameters may be different as mentioned above.

Straightforward calculation of the differential cross-section for $e^-q \to e^*q$ yields [5,15]

$$\begin{aligned}
\frac{d\sigma}{dt}(e^-q \to e^*q; \hat{s}) &= \frac{\pi\alpha^2}{\Lambda^{*2}\hat{s}^2}\{[(2\hat{s} - m_{e^*}^2)(m_{e^*}^2 - t) - 2\hat{s}^2] \\
&\times [\frac{Q_q^2}{t} + \frac{4Q_qv_q(1-2\sin^2\theta_W)}{\sin^2 2\theta_W}\frac{1}{t-m_Z^2} + \frac{4(v_q^2+a_q^2)(1-2sin^2\theta_W)^2}{\sin^4 2\theta_W}\frac{t}{(t-m_Z^2)^2}] \\
&\pm 4m_{e^*}^2(m_{e^*}^2 - t - 2\hat{s}) \\
&\times [\frac{Q_qa_q(1-2\sin^2\theta_W)}{\sin^2 2\theta_W}\frac{1}{t-m_Z^2} + \frac{2v_qa_q(1-2sin^2\theta_W)^2}{\sin^4 2\theta_W}\frac{t}{(t-m_Z^2)^2}]\}
\end{aligned} \tag{15}$$

The notation is as in eqs.(6) and (14) wherefrom the relevant couplings to the γ and Z can be read off. Furthermore, $\hat{s}$ and t are the usual Mandelstam variables for the subprocess $eq \to e^*q$, and the plus (minus) sign refers to quarks (antiquarks). The integrated production cross-section is then given by

$$\sigma_{inel}(e^-p \to e^*X) = \int_{x_{min}}^1 dx \int_{t_{max}}^{t_{min}} dt \sum_q q(x, Q^2)\frac{d\sigma}{dt}(e^-q \to e^*q; xs), \tag{16}$$

where $q(x,Q^2)$ are the quark distribution functions of the proton, and the sum runs over quarks and antiquarks. As parametrizations we have used set I of ref.[13] with $Q^2 = -t$ as the evolution scale. For the integration boundaries in eq.(15) we take

$$t_{min} = -Q_0^2 \quad , \quad t_{max} = -(sx - m_{e^*}^2) \quad , \quad x_{min} = (m_{e^*}^2 + Q_0^2)/s. \tag{17}$$

The cut-off $Q_0^2 = 5\ GeV^2$ is imposed in order to stay within the region of validity of the parton model. Correspondingly, eq.(15) provides an estimate for *inelastic* e^* production ($X \neq p$).

However,since the photon is massless, the low-t region may also yield a sizeable contribution to the total cross-section. Indeed, it has been shown in ref.[15] that at HERA energies elastic production $ep \to e^*p$ is as strong as inelastic production. We have therefore estimated elastic production in the energy range of LEP-LHC. Using the formulas provided in ref.[15], the differential cross-section for $ep \to e^*p$ can be written in the form

$$\frac{d\sigma}{dt}(ep \to e^*p) = \frac{\pi\alpha^2}{2\Lambda^{*2}} \frac{1}{(s-m_p^2)^2} \{G_M^2(t) \frac{(2m_{e^*}^2+t)(t-m_{e^*}^2)}{t}$$
$$+[G_E^2(t) - \frac{t}{4m_p^2}G_M^2(t)][(m_{e^*}^2 - t)(4s + t - 4m_p^2 - \frac{4m_p^2 m_{e^*}^2}{t}) - 4(s - m_p^2)^2]\frac{4m_p^2}{t(4m_p^2-t)}\}, \tag{18}$$

where

$$G_E(t) \simeq G_M(t)/2.79 \simeq (1 - t/0.71\ GeV^2)^{-2} \tag{19}$$

are the measured electric and magnetic form factors G_E and G_M of the proton. The elastic production cross-section is then obtained by integrating eq.(18) over t with the boundaries

$$t_{\substack{\min\\ \max}} = m_{e^*}^2 - \frac{s - m_p^2}{2s}\{s + m_{e^*}^2 - m_p^2 \mp \sqrt{(s - m_{e^*} - m_p^2)^2 - 4m_{e^*}^2 m_p^2}\}. \tag{20}$$

Fig. 7 shows the total production cross-sections

$$\sigma_{tot}(e^-p \to e^*X) \simeq \sigma_{incl}(e^-p \to e^*X) + \sigma_{el}(e^-p \to e^*p) \tag{21}$$

as a function of m_{e^*} for the two ep options specified in eq.(1). Also displayed are the elastic and inelastic contributions. A large fraction of the e^* events is expected to contain an electron and a photon in the final state coming from the decay $e^* \to e\gamma$. The prospects for detecting the $e\gamma$ signal in the background from $ep \to eX$ and $ep \to \nu X$ have been studied in ref.[16] for inelastic e^* production at HERA. Monte Carlo simulations show that it should be rather easy to separate signal and background by appropriate cuts in various kinematical variables such as the total visible mass of the event and the transverse momentum in the event plane. Furthermore, the e^* mass seems to be quite well reconstructable. It was concluded that $\sigma_{inel}(ep \to e^*X) \times B(e^* \to e\gamma) \simeq 0.2\ pb$ is the limit of observability for an integrated luminosity of 200 pb^{-1} yielding an statistical significance of $2-3$ standard deviations [16]. Hence, it may be somewhat optimistic but it is not unreasonable to consider $\sigma_{tot}(ep \to e^*X) \simeq 0.01(0.1)\ pb$ as the smallest observable cross-section at the 1.4(1.8) TeV option at LEP-LHC. Under this assumption we find from Fig. 7 that one can reach e^* masses up to

$$m_{e^*} \simeq 1\ TeV \tag{22}$$

at both ep energies. It should be emphasized, however, that the above estimate holds for $\Lambda^* = m_{e^*}$. For example, for $\Lambda^* \simeq 5\ TeV > m_{e^*}$ the detection limit drops to $m_{e^*} \simeq 650(200)\ GeV$ at $\sqrt{s} = 1.4(1.8)\ TeV$ and $L = 10^{32}(10^{31})\ cm^{-2}s^{-1}$, attributing clear preference to high luminosity.

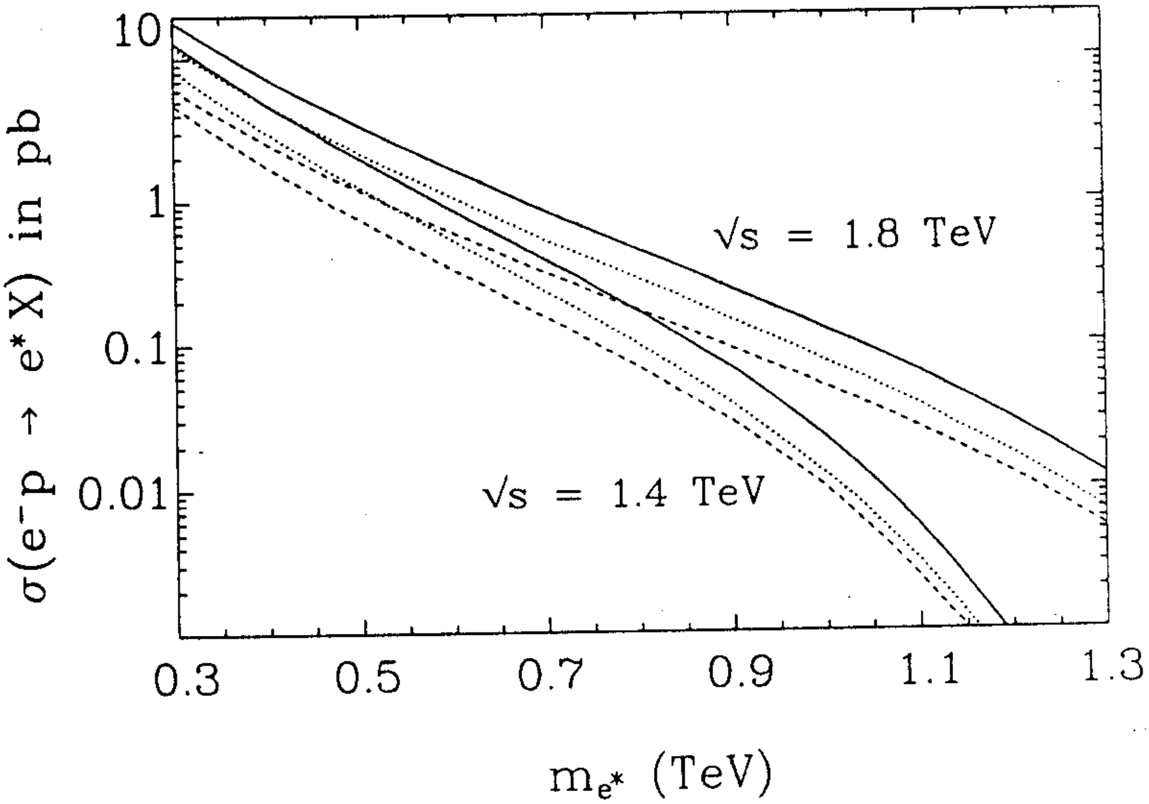

Fig. 7 Excited electron production in ep collisions al LEP-LHC. Shown are the cross-sections for elastic production $ep \to e^*p$ (dashed), inelastic production $ep \to e^*X$ (dotted), and the sum of both (full line).

4. SUMMARY

We have studied the possibilities to search for eq contact interactions and an excited electron in ep collisions at LEP-LHC. Contact terms can be tested by measurements of inclusive cross-sections and asymmetries in $ep \to eX$. Concentrating on the $\sqrt{s} = 1.4\ TeV$, $L = 10^{32}\ cm^{-2}s^{-1}$ ep option we have estimated the sensitivity to the compositeness Λ_{eq} which governs the strength of contact terms. Our estimates are based on considerations of statistical errors corresponding to a total integrated luminosity of 1 fb^{-1}, that is $500 pb^{-1}$ per initial state for unpolarized $e^{\mp}p$ collisions and 250 pb^{-1} per initial state for polarized $e^{\mp}_{L,R}p$ collisions. The results can be summarized as follows. Measurements of NC cross-sections are expected to be sensitive to contact interactions up to

$$\Lambda_{eq} \simeq (9 - 16)\ TeV, \tag{23}$$

depending on the helicity structure of the contact terms, and assuming the favorable case $\eta_{ab} \geq 0$, η_{ab} being the effective couplings in eq.(7). If one allows for systematic errors of the same size as the statistical errors and adds both linearly, it should still be possible to reach

$$\Lambda_{eq} \simeq (7-12)\,TeV. \tag{24}$$

Furthermore, asymmetry measurements are sensitive to contact interactions up to

$$\Lambda_{eq} \simeq (8-14)\,TeV, \tag{25}$$

if statistical errors dominate. Comparison of Tables 3 and 4 indicates that cross-section measurements are slightly more sensitive to certain helicity combinations than asymmetry measurements. For other contact terms just the opposite is true. In addition, asymmetries turn out to be very useful for determining the chiral structure of contact interactions which might be discovered. We also find that luminosity is more important in these searches than energy (similarly as in searches for Z' bosons [14]) and hence the limits one can expect for the $\sqrt{s} = 1.8\,TeV$, $L = 10^{31}\,cm^{-2}s^{-1}$ ep option are considerably lower than the ones quoted above.

Excited electrons are mainly produced in the process $ep \to e^*X$. We expect roughly equal cross-sections for inelastic ($X \neq p$) and elastic ($X = p$) production. Assuming that 10 events per year are sufficient for detection, one can reach e^* masses up to

$$m_{e^*} \simeq 1\,TeV \tag{26}$$

at both the 1.4 and 1.8 TeV ep option. Thus, here is one case where a higher ep energy can compensate for a lower luminosity. However, it should be noted that this trade-off is not true generally. In particular, it depends on the relation of Λ^* and m_{e^*} (see eq.(13)). If $\Lambda^* > m_{e^*}$, in contrast to our assumption $\Lambda^* = m_{e^*}$, the 1.4 TeV option is again clearly preferred.

References

[1] W. Buchmüller, Acta Phys. Austriaca Suppl. XXVII (1985) 517;
M.E. Peskin, Proc. of the Int. Symp. on Lepton and Photon Interactions at High Energies, Kyoto, 1985, eds. M. Konuma and K. Takahashi (Kyoto University, Kyoto, 1986) p. 713.

[2] H. Harari, Proc. of the 5th Topical Workshop on Proton-Antiproton Collider Physics, Saint-Vincent, Aosta Valley, 1985, ed. M. Greco (World Scientific Pub. Co., Singapore, 1985) p. 429.

[3] S. Komamiya, Proc. of the Int. Symp.on Lepton and Photon Interactions at High Energies, Kyoto, 1985, eds. M. Konuma and K. Takahashi (Kyoto University, Kyoto, 1986) p. 612.

[4] R.N. Cahn and H. Harari, Nucl. Phys. B176 (1980) 135;
D. Wyler, Proc. of the 23rd Int. Conf. on High Energy Physics, Berkeley, 1986, ed. S.C. Loken (World Scientific Pub. Co., Singapore, 1986)p. 438.

[5] G. Altarelli, B. Mele and R. Rückl, Proc. of the ECFA-CERN Workshop on a Large Hadron Collider in the LEP Tunnel, Lausanne and CERN, 1984, ed. M. Jacob (ECFA 84/85, CERN 84-10, Geneva, 1984) p. 551;
J.A. Bagger and M.E. Peskin, Phys. Rev. D31 (1985) 2211 and Erratum D32 (1985) 1260.

[6] G. Brianti, Vol. I of these Proceedings, p. 6.

[7] J. Ellis and F. Pauss, Vol. I of these Proceedings, p. 80.

[8] E.J. Eichten, K.D. Lane and M.E. Peskin, Phys. Rev. Lett. 50 (1983) 811.

[9] C.J.C. Burges and H.J. Schnitzer, Nucl. Phys. B228 (1983) 464 and Phys. Lett. 134B (1984) 329;
C.N. Leung, S.T. Love and S. Rao, Z. Phys. C31 (1986) 433;
W. Buchmüller and D. Wyler, Nucl. Phys. B268 (1986) 621.

[10] C. Rubbia, Proc. of the Int. Symp.on Lepton and Photon Interactions at High Energies, Kyoto, 1985, eds. M. Konuma and K. Takahashi (Kyoto University, Kyoto, 1986) p. 242.

[11] R. Rückl, Phys. Lett. 129B (1983) 363 and Nucl. Phys. B234 (1984) 91.

[12] F. Cornet, to appear in Proc. of the 25th Int. Winter Meeting on Fundamental Physics, Sevilla (1987).

[13] D.W. Duke and J.F. Owens, Phys. Rev. D30 (1984) 49.

[14] F. Cornet and R. Rückl, Vol. II of these Proceedings.

[15] K. Hagiwara, D. Zeppenfeld and S. Komamiya, Z. Phys. C29 (1985) 115.

[16] R.J. Cashmore et al., Phys. Rep. 122 (1985) 275.

[17] F.M. Renard, Phys. Lett. 116B (1982) 264;
F. del Aguila, A. Méndez and R. Pascual, Phys. Lett. 140B (1984) 431;
M. Suzuki, Phys. Lett. 143B (1984) 237.